

**SIMULATION OF THE VIRGINIA TECH FIRE
RESEARCH LABORATORY USING LARGE
EDDY-SIMULATION WITH MIXTURE FRACTION
CHEMISTRY AND FINITE VOLUME RADIATIVE HEAT
TRANSFER**

by

J.E. Floyd
Building and Fire Research Laboratory
National Institute of Standards and Technology
Gaithersburg, MD 20899, USA

C. Wieczorek and U. Vandsburger
Department of Mechanical Engineering
Virginia Polytechnic Institute and State University
Blacksburg, VA 24061, USA

Reprinted from Proceedings of Interflam '01, Ninth International Fire Science and Engineering Conference. Volume 1. September 17 – 19, 2001, Edinburgh, Scotland. Interscience Communications Ltd., London, United Kingdom, 767-778 pp, 2001.

NOTE: This paper is a contribution of the National Institute of Standards and Technology and is not subject to copyright.



NIST

National Institute of Standards and Technology
Technology Administration, U.S. Department of Commerce

SIMULATION OF THE VIRGINIA TECH FIRE RESEARCH LABORATORY USING LARGE EDDY-SIMULATION WITH MIXTURE FRACTION CHEMISTRY AND FINITE VOLUME RADIATIVE HEAT TRANSFER

Jason E. Floyd

Building and Fire Research Laboratory
National Institute of Standards and Technology
Gaithersburg, MD 20899, USA

Christopher J. Wieczorek and Uri Vandsburger
Department of Mechanical Engineering
Virginia Polytechnic Institute and State University
Blacksburg, VA 24061, USA

SUMMARY

A mixture fraction based combustion model and a finite volume radiation transport model have been added to the Fire Dynamics Simulator (FDS) developed at the National Institute of Standards and Technology. Computations of three propane fire experiments, 90 kW, 270 kW, and 440 kW, in a one-half scale ISO 9705 compartment are made with the new models. The computational results are compared to data collected at the Virginia Tech Fire Research Laboratory (VTFRL).

INTRODUCTION

The simulation of fires using computational fluid dynamics (CFD) is a challenging endeavor. It is difficult to couple the combustion chemistry that occurs at very small length scales with the resolvable hydrodynamic field. There is also the added complexity of coupling the heat transfer occurring on the convective time scale with that occurring on the radiative time scale. It is possible to create both a combustion model that tracks the significant species required to calculate the heat release rate and a heat transfer model to compute the convective and radiative heat transfer to surfaces; however, for most cases it is too computationally expensive to construct a grid fine enough to resolve individual flame sheets or to completely solve the radiative flux at each time step. Methods, therefore, are needed to model the combustion chemistry at the length scales of the resolvable flow field and to compute the radiative heat transfer in a computationally efficient manner.

FDS v1.0¹ contained two simple models for handling combustion and radiative heat transfer. Combustion was modeled by injecting Lagrangian particles into the flow that represented

small quanta of fuel. The particles would emit heat at a constant rate for a user defined burnout time. Oxygen would be depleted by burning particles. Radiation heat transfer was modeled by using a Monte-Carlo ray tracing method. A subset of the burning particles would be selected and a ray tracing to all visible wall cells performed. The summation of all the rays from the selected particles would then be scaled by the total number of burning particles.

These methods were relatively simple to implement and were not overly computationally intensive. However, they have a number of disadvantages for fire safety analysis of compartments. One is that the particle method does not yield any information about combustion products. To do so with this method would require an additional species equation for each product and quickly consume computational resources. A second is that the ray tracing method as implemented does not account for surface to surface radiation and without knowledge of species cannot properly account for hot gas to surface interactions. These additional interactions become significant for compartment fires that are large with respect to the size of the compartment. As with the particle method, extending the ray tracing method to include wall cells and gas cells would add a significant computational burden. The result of these disadvantages is that for many compartment fires, FDS would predict too large of a heat release rate inside the compartment and predict too little heat transfer to the walls resulting in high gas temperature predictions².

To overcome the limitations of the initial models, continuing development of FDS v1.0 has added a mixture fraction combustion model^{3,4} and a finite volume radiation heat transfer model⁵. A mixture fraction model, which uses one scalar variable to represent the local concentration of fuel, air, and combustion products, has been developed that allows the flame sheet to ‘spread’ over a large grid cell, allowing the mixture fraction to be used at many different length scales. The new radiation heat transfer model uses information from the mixture fraction to determine the radiative field in the computational domain. Both of these models will require validation against experimental data.

One set of data being used for this validation is a set of propane fire experiments in a scaled ISO 9705 compartment performed at Virginia Tech to develop state relations for combustion products such as CO. Instrumentation for the compartment consists of two rakes of aspirated thermocouples, one inside the compartment and one in the doorway, a rake in the doorway containing both bi-directional velocity probes and gas sampling lines which can be moved across the width of the doorway, and heat flux gauges located both inside and outside the compartment.⁶

FDS with its new sub-models, was used to simulate three experiments performed at the VTFRL. Comparisons between FDS predictions and the VTFRL data are made. Conclusions are drawn about the performance of FDS with the new models and avenues of future improvement are discussed.

NEW FDS MODELS

Mixture Fraction Chemistry Model

FDS solves the “low Mach number” form of the Navier-Stokes equations¹ for a multiple species fluid. These equations are obtained by filtering out pressure waves from the

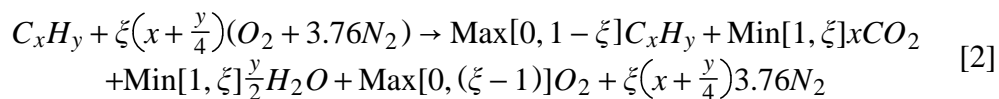
Navier-Stokes equations, resulting in a set of conservation equations valid for low-speed, buoyancy driven flow. The equations allow for large variations in density but not pressure. These equations are discretized in space using second order central differences and in time using an explicit, second order, predictor-corrector scheme. For very small scale diffusion flames, such as a small burner, it is feasible to create a simulation capable of being run on a modestly powered computing platform that is detailed enough in both length scales and time scales to directly capture the combustion processes. However, for the large scale problems of interest to the fire safety community this is not feasible.

Overcoming the limitations of computational power requires that the chemistry and physics of combustion must be simplified. One simple method of coupling the combustion process with the flow field is to track three species: fuel, oxygen, and nitrogen. Since the time scales of the convective processes are much longer than the time scales of the combustion processes, infinite reaction rate chemistry can be assumed. Note, however, that this method requires solving for three species, and that more species would be required to handle combustion products. Since every species being tracked adds to the computational time, this method is not particularly desirable. The observation can be made, however, that to track both fuel and oxygen when assuming an infinite reaction rate is redundant if the local temperature is not considered. Since neither fuel nor oxygen can coexist under those assumptions, if fuel is present there can be no oxygen and vice-versa. Thus, the above method could be simplified further by replacing all the species with a single species that represents the amount of fuel or oxygen present in any given location.

One scalar parameter that can be used to represent the local concentration of fuel or oxygen is the mixture fraction. If F is defined as fuel, O is defined as oxygen, Y is defined as a mass fraction, Y_O^∞ as the ambient oxygen mass fraction, Y_F^I as the fuel mass fraction in the fuel stream, ν is the moles required for complete combustion and w the molecular weight, the mixture fraction, Z , is defined as⁴:

$$Z = \frac{sY_F - (Y_O - Y_O^\infty)}{sY_F^I + Y_O^\infty}; \quad s = \frac{\nu_O w_O}{\nu_F w_F} \quad [1]$$

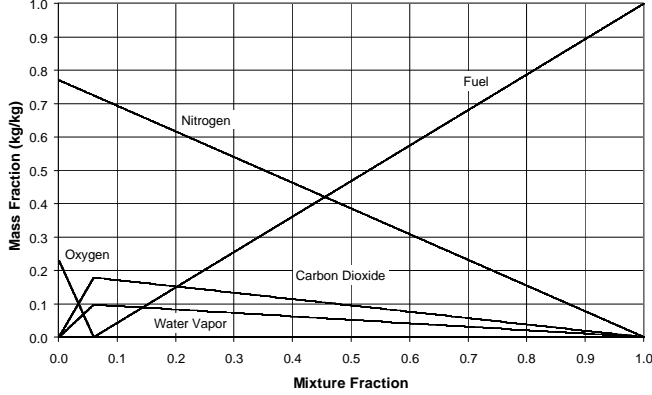
In its traditional implementation, mixture fraction chemistry assumes that fuel and oxygen cannot co-exist. That is, it uses an infinite reaction rate and assumes that fuel and oxygen will react at any temperature. Thus, the mixture fraction at all points in the computational domain, in essence represents a ‘post-combustion’ value, i.e. only products are present at any location in the computational domain. This is more easily seen in the following. Assume that a generic hydrocarbon fuel is being burned in air. The chemical reaction, assuming no products of incomplete combustion, for this is:



Where ξ is a parameter varying from 0 to ∞ that dictates the amount of air supplied.

Using Equation 1, the mass fractions of the products in Equation 2 can be plotted as a function of Z . As ξ varies from ∞ to 0, Z will vary from 0 to 1, and a series of state

relationships for the species can be expressed in terms of the mixture fraction. In this idealization, the mixture fraction represents many species in the simulation. For example, if the fuel species is propane, the idealized state relationships shown in Figure 1 are obtained.



1. Propane State Relations

With this representation the flame sheet is defined to exist at the point where both fuel and oxygen disappear as products. The mixture fraction corresponding to this point is designated Z_F and this point is equivalent to the reaction shown in Equation 2 with $\xi=1$. This region is a two dimensional surface, and for larger scale simulations is difficult to resolve. To implement the mixture fraction an expression for the local heat release rate as a function of the mixture fraction must be developed.

This is done rather simply. Combustion of fuel consumes oxygen. Since the mixture fraction yields information about the local oxygen concentration, we need only determine an expression for the oxygen consumption rate based on the mixture fraction and multiply it by the heat of combustion to yield the local heat release rate. Consider the transport equations for the conserved scalar Z and for oxygen where D is the turbulent diffusion coefficient which for a large eddy simulation is calculated from Smagorinsky's theory, ρ is the local gas density, and \dot{m}_O is the local mass loss rate per unit volume of oxygen, e.g. oxygen consumption during combustion.

$$\rho \frac{DZ}{Dt} = \nabla \cdot \rho D \nabla Z \quad [3]$$

$$\rho \frac{DY_O}{Dt} = \nabla \cdot \rho D \nabla Y_O + \dot{m}_O \quad [4]$$

If the derivatives for oxygen in Equation 4 are expressed in terms of mixture fraction using the chain rule, diffusion is assumed constant with respect to species, and Equation 3 is multiplied by $\frac{dY_O}{dZ}$, then rearranging the equations will yield

$$-\dot{m}_O = \nabla \cdot \rho D \frac{dY_O}{dZ} \nabla Z - \frac{dY_O}{dZ} \nabla \cdot \rho D \nabla Z \quad [5]$$

With Equation 5 one can now determine the local mass loss rate of oxygen as a function of the mixture fraction. At first glance, Equation 5 appears to be rather complex. However, its meaning can be simplified. It can be seen in Figure 1 that $\frac{dY_O}{dZ}$ at any point in the computational domain is either zero or a constant depending its relation to Z_F . If the computational domain is divided into the two regions of $Z \leq Z_F$ and $Z > Z_F$, then Equation 5 can be integrated over these two regions while applying the divergence theorem. Since the $\frac{dY_O}{dZ}$ term equals zero in the region $Z > Z_F$, this region can be ignored. The end result is that the

mass loss rate of oxygen is constructed as a function of the mixture fraction diffusion across the flame surface as shown below:

$$\int \dot{m}_O \partial V = -\frac{dY_O}{dZ} \int_{Z=Z_F} \rho D \nabla Z \cdot \vec{n} \partial S \quad [6]$$

Since oxygen is a function of only the mixture fraction, this is equivalent to saying that the heat release rate is a function of the oxygen gradient across the flame sheet. In fact due to the diffusion constant in the expression and the assumption of infinite reaction rates, Equation 6 states that the heat release rate is due solely to the diffusion of oxygen across the flame, which is calculated by the hydrodynamic solver. Thus, by tracking only the mixture fraction and by evaluating Equation 6 at each time step, it is possible to computationally model a fire allowing large grid sizes at a reasonable computational cost.

Finite Volume Radiation Transport Model

Calculating the correct spatial distribution and magnitude of the heat release rate is only one aspect of a successful fire model. Computing how that energy is then distributed throughout the computational domain is also required. In FDS the convective and conductive transfer of heat is handled by the hydrodynamics solver. A separate solver is required for the radiative transfer of heat. In FDS v1.0, the radiative fluxes were computed with a Monte-Carlo style ray-tracing from cells containing burning fuel to the walls. The model neglected gas to gas and wall to wall interactions, and thus, did not fare well with compartment scenarios with hot gas layers or surfaces. To remedy this the original Monte-Carlo style radiation model was changed to a Finite Volume Method⁵. This method is derived from the radiative transport equation for a non-scattering gray gas.

$$\hat{s} \cdot \nabla I(x, \hat{s}) = \kappa(x)[I_b(x) - I(x, \hat{s})] \quad [7]$$

$I(x, \hat{s})$ is the radiation intensity, $I_b(x)$ is the blackbody radiation intensity, $\kappa(x)$ is the absorption coefficient, and \hat{s} is the unit normal direction vector. Implementing this equation in a large eddy simulation requires determining how to specify the absorption coefficient, κ , and how to model the source term $I_b(x)$.

The absorption coefficient, κ , for a gray gas model is a function of the local species concentration, the local temperature, and the pathlength over which the radiation heat transfer occurs⁸. The local species concentrations for fuel, CO₂, and water vapor are defined by the local mixture fraction and soot is currently being assumed to be produced at a magnitude proportional to the local CO₂ yield based on experimentally measured yields¹¹. Temperature is also known from the hydrodynamic solution. The pathlength, however, is not easily determined for most fire scenarios. To obtain κ , RADCAL⁷ is run at the start of a computation to generate a two dimensional array mapping κ as a function of temperature and mixture fraction. The pathlength is assumed to be related to the computational domain's lengthscale.

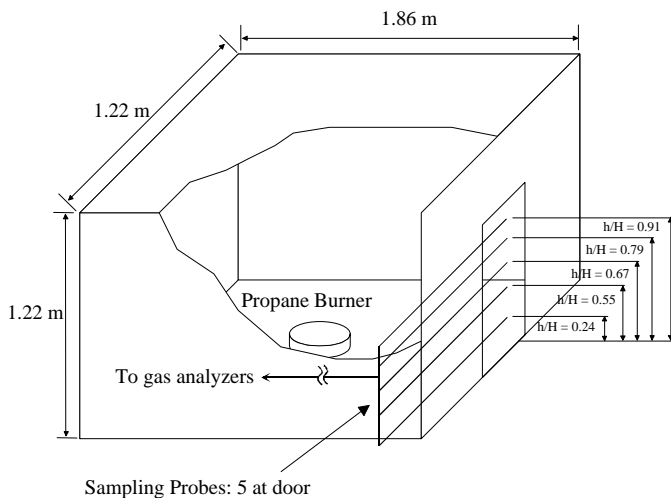
The blackbody term, I_b , is easily defined in cells without combustion. For these cells the term is defined below where T is the local temperature and σ is the Stefan-Boltzman constant:

$$I_b = \frac{\sigma T^4}{\pi} \quad [8]$$

In computational cells with combustion occurring, specifying I_b is more difficult. In general, for most scenarios the grid size is > 10 cm which is too coarse to actually resolve the flame. Because of this, the cell averaged temperatures in those cells where combustion is occurring will tend to be lower than the actual flame temperature. Since the blackbody term uses temperature to the fourth power, use of this lower temperature will underpredict the radiative emission from the combustion zone. Thus, in cells with combustion, the source will need to be corrected to account for this. Determining how to deal with the blackbody term for large grid cells is still under investigation.

VTFRL COMPARTMENT

The Virginia Tech Fire Research Laboratory is currently involved in a multi-year research project to examine the production and transport of carbon monoxide in compartment fires⁶. The goal of this project is to create a better understanding of how CO is generated in a compartment fire and then transported to other locations distant from the fire where it is liable to cause death or injury⁸. The current phase of this project involves measuring combustion product formation resulting from propane fires in a scaled ISO 9705 compartment.



2. VTFRL Test Compartment

The experiments were performed in a length and Froude number scaled ISO 9705 standard compartment, shown in Figure 2. The wall thickness of the compartment was scaled to preserve heat transfer similarity and the doorway was scaled to preserve dynamic flow similarity. The compartment, constructed of a steel sheet over a steel skeleton, is lined on the interior with 25.4 mm thick fiberboard. The interior compartment dimensions are 1.17 m wide by 1.78 m deep by 1.17 m high. Scaling of the doorway resulted in a baseline door that was 0.33 m wide and 0.82 m high. Two other doorway sizes were used which represent a partially opened standard door, half the width of the baseline, and a double door, twice the width of the baseline. To promote the formation of an upper layer, a 0.4 m deep soffit was used. The doorway was located under a fume hood to ensure the safety of the experimentalists.

Data collected during the tests included compartment temperatures, doorway temperatures, velocities, concentrations of CO_2 , CO , O_2 , and unburned hydrocarbons (UHC), and total heat flux. Temperatures in the front corner of the compartment and along the edge of the doorway were each measured using a rake of eight aspirated thermocouples designed based on the recommendations of Blevins⁹ with estimated uncertainties of 7 % in the upper layer and 25 %

in the lower layer based on an aspiration velocity of 25 m/s. Velocities were measured with five bi-directional velocity probes on a movable stand with an estimated uncertainty of 4 %; four located in the out-flowing region of the doorway and one in the in-flowing region of the doorway. Gas samples were taken by a rake of five sampling lines located at the same location as the velocity probes. Errors in the gas measurements have been determined to be 10 % for CO and UHC, 5 % for O₂, and 7 % for CO₂.¹⁰ Six heat flux gauges were placed in and around the compartment: two gauges on the inside wall of the compartment next to the doorway, two gauges outside the doorway at the floor level along the doorway centerline, and two gauges approximately 1.5 m from the compartment looking in the doorway. Heat flux uncertainty are estimated to be 5 % based on repeatability of the measurements. In all 26 tests were run with the three different door sizes.

EXPERIMENTS MODELED

Three baseline door experiments were modeled with FDS. The experiments modeled were a 90 kW fire, a 270 kW fire, and a 440 kW fire. Since the current implementation of the mixture fraction model does not include minor species such as CO, the heat of combustion for propane was reduced for the 270 kW and 440 kW fire to account for the production of CO. This was done by using the measured data from the test to determine the combustion efficiency inside the compartment and reducing the heat of combustion accordingly. It was hoped that this would limit FDS's overprediction of the heat release rate due to its assumption of ideal combustion while ensuring the correct fuel mass flow rate out of the burner. Soot production was set to a soot to fuel mass ratio of 0.024 g/g burned¹¹.

Each of the three tests used the same input geometry. The models all consisted of a computational domain 1.17 m x 2.50 m x 1.40 m with 32 x 64 x 40 nodes, or the size of the compartment plus 0.69 m beyond the doorway. The noding used has a maximum grid spacing of 0.04 m which is below the flow solver requirement of 0.07 m for the 440 kW fire¹². All of the wall surfaces were defined as the insulating material used inside the compartment. The actual thermal properties of the material were used with the exception of the heat capacity. The wall heat capacity in the input file was reduced by an order of magnitude. This was done to reduce the computational time required to reach steady state conditions inside the compartment. Since the other material properties were not changed, the steady state heat transfer through the walls was not affected. The circular burner was approximated with rectangular grids.

COMPARISONS WITH DATA

The first test modeled was a 90 kW fire. During this test a stable two-layer system developed inside the compartment. Flamelets were seen to be exiting the compartment in the top few centimeters of the doorway. Only minimal CO production was observed in the doorway during this test. Comparison between the measured test data with the FDS predictions are shown in Table 1 below. The velocity and species concentrations are for the doorway centerline. The temperatures are given as the change from the initial temperature which was near 285 K for all three tests.

First, a comment regarding measurements. The measured door temperatures indicate that Door TC 1 had a higher temperature than TC 2 which was 0.1 m above it. The authors

believe that the actual temperature at the lowest door TC in this test did not rise above the ambient. A bare bead TC that was present outside the door at the floor level of the compartment, but not visible to walls of the compartment, showed a temperature increase of only a few degrees. Since the ambient atmosphere contains small amounts of water vapor and CO₂ and the distance from the bare bead TC to the doorway was on the order of 1 m, it is not possible that the incoming air could heat up that much in that short amount of transport time to the door. It is hypothesized that being closer to the floor this lowest TC was preferentially heated by radiative emission from the floor.

1. Results for the 90 kW

| Parameter | VTFRL | FDS | Parameter | VTFRL | FDS |
|------------|-----------------------|-----------------------|------------------------|--------|--------|
| Door TC 1 | 29 °C | 5 °C | Room TC 1 | 191 °C | 134 °C |
| Door TC 2 | 14 °C | 1 °C | Room TC 2 | 219 °C | 171 °C |
| Door TC 3 | 30 °C | 19 °C | Room TC 3 | 255 °C | 247 °C |
| Door TC 4 | 44 °C | 106 °C | Room TC 4 | 291 °C | 438 °C |
| Door TC 5 | 348 °C | 365 °C | Room TC 5 | 585 °C | 529 °C |
| Door TC 6 | 559 °C | 473 °C | Room TC 6 | 603 °C | 544 °C |
| Door TC 7 | 552 °C | 493 °C | Room TC 7 | 617 °C | 551 °C |
| Door TC 8 | 227 °C | 409 °C | Room TC 8 | 625 °C | 558 °C |
| Door Vel 1 | 4.4 m/s | 3.3 m/s | Door O ₂ 1 | 14.6 % | 13.9 % |
| Door Vel 2 | 3.3 m/s | 2.4 m/s | Door O ₂ 2 | 15.7 % | 14.1 % |
| Door Vel 3 | 2.1 m/s | 1.8 m/s | Door O ₂ 3 | 18.4 % | 14.6 % |
| Door Vel 4 | 0.72 m/s | 1.4 m/s | Door O ₂ 4 | 20.3 % | 16.7 % |
| Door Vel 5 | -0.54 m/s | -0.75 m/s | Door O ₂ 5 | 21.0 % | 21.0 % |
| Room HF 1 | 29 kW/m ² | 26 kW/m ² | Door CO ₂ 1 | 3.5 % | 3.8 % |
| Room HF 2 | 25 kW/m ² | 24 kW/m ² | Door CO ₂ 2 | 2.8 % | 3.7 % |
| Door HF 1 | 8.4 kW/m ² | 7.7 kW/m ² | Door CO ₂ 3 | 1.3 % | 3.4 % |
| Door HF 2 | 3.6 kW/m ² | 4.1 kW/m ² | Door CO ₂ 4 | 0.2 % | 2.2 % |
| | | | Door CO ₂ 5 | 0.0 % | 0.0 % |

Overall, FDS predicted well the measured quantities. With the exception of Door TC's 4 and 8 the FDS predicted temperatures in the doorway match the measured data within the measured uncertainty. Based on the temperature, velocity, and gas concentration profiles it would seem that the error in Door TC 4 results from FDS predicting a thicker upper layer than existed in the test; this is most likely due to the nodding resolution resulting in excessive mixing at the layer interface. At Door TC8 the exiting gas stream formed a recirculation zone at the upper edge of the doorway which entrained ambient air. This zone included TC 8; hence, its lower temperature. FDS did predict this behavior, but did not correctly predict the magnitude of the temperature decrease. Inside the fire room, FDS predictions with the exception of Room TC 4 are within 10 % of the measured quantities. FDS velocity predictions, while matching the trend in the data, do not match as well as the temperatures in magnitude. FDS is underpredicting the upper velocities by 30-40 % and overpredicting the incoming velocity by 40 %. However, since FDS is predicting too large of an upper layer, if FDS were correctly predicting the overall mass exchange in the doorway, conservation of mass would dictate that upper velocities be underpredicted and lower velocities be overpredicted. This is indeed the trend in the FDS predictions. FDS predictions of the heat

flux gauge response are within 10 % of the measured response. Lastly, FDS correctly predicts the gas concentrations at the very top of the doorway, however, due to the enhanced mixing of the layer interface, the gas concentrations in the remainder of the upper layer are not as well predicted.

The second test modeled was a 270 kW fire. During this test small concentrations of CO were measured. Significant external burning occurred during this test and flames inside the compartment nearly reached the floor. Table 2 below gives the FDS results along with the corresponding measured data. During this test the heat flux gauges inside the compartment reached or exceeded their maximum range and therefore are not usable for comparisons. Also, since FDS tracks only CO₂, the measured data for the compartment is shown as CO₂ and (CO₂+CO). In this manner the total burned carbon flux through the doorway can be compared.

2. Results for the 270 kW Fire

| Parameter | VTFRL | FDS | Parameter | VTFRL | FDS |
|------------|----------------------|-----------------------|------------------------|-------------|---------|
| Door TC 1 | 122 °C | 30 °C | Room TC 1 | 467 °C | 1090 °C |
| Door TC 2 | 66 °C | 125 °C | Room TC 2 | 528 °C | 1120 °C |
| Door TC 3 | 149 °C | 421 °C | Room TC 3 | 721 °C | 1150 °C |
| Door TC 4 | 273 °C | 737 °C | Room TC 4 | 913 °C | 1170 °C |
| Door TC 5 | 801 °C | 935 °C | Room TC 5 | 959 °C | 1190 °C |
| Door TC 6 | 982 °C | 976 °C | Room TC 6 | 1062 °C | 1200 °C |
| Door TC 7 | 1019 °C | 958 °C | Room TC 7 | 1088 °C | 1220 °C |
| Door TC 8 | 985 °C | 695 °C | Room TC 8 | 1083 °C | 1240 °C |
| Door Vel 1 | 5.2 m/s | 4.9 m/s | Door O ₂ 1 | 3.8 % | 3.2 % |
| Door Vel 2 | 4.0 m/s | 4.7 m/s | Door O ₂ 2 | 6.7 % | 2.6 % |
| Door Vel 3 | 2.7 m/s | 3.7 m/s | Door O ₂ 3 | 13.8 % | 3.2 % |
| Door Vel 4 | 1.4 m/s | 2.9 m/s | Door O ₂ 4 | 18.8 % | 3.7 % |
| Door Vel 5 | -1.3 m/s | -0.13 m/s | Door O ₂ 5 | 20.6 % | 16.9 % |
| Room HF 1 | N/A | 259 kW/m ² | Door CO ₂ 1 | 8.5 (9.3) % | 9.7 % |
| Room HF 2 | N/A | 228 kW/m ² | Door CO ₂ 2 | 7.2 (7.7) % | 10.1 % |
| Door HF 1 | 63 kW/m ² | 82 kW/m ² | Door CO ₂ 3 | 3.7 (3.8) % | 9.7 % |
| Door HF 2 | 36 kW/m ² | 41 kW/m ² | Door CO ₂ 4 | 1.0 (1.1) % | 9.5 % |
| | | | Door CO ₂ 5 | 0.1 (0.1) % | 2.1 % |

Similar observations can be made for this test as for the 90 kW test. FDS has again predicted a thicker upper layer than was measured. This resulted in the higher temperatures predictions for Door TC's 2-4. The upper doorway temperatures are well predicted. Inside the fire room, FDS temperature predictions are high in the lower layer by 50 %. The upper layer is high by 20 %. FDS also predicts a much larger region of completely oxygen depleted gas in the upper layer of the doorway. These two items combined would suggest that FDS is allowing too much combustion to occur inside the fire room, causing an increase in fire room temperatures and an overly oxygen depleted exit flow through the doorway. This can also be seen in the large error in burned carbon for gas locations 3 and 4. This could result from numerical errors due to the nodding and may also result in part to the assumption of ideal combustion in the current implementation of the mixture fraction; e.g., there was no

accounting for soot. Lastly, FDS is overpredicting the two functioning heat flux gauges by 30 %. However, as FDS is overpredicting the fire room upper layer temperatures by 200 °C, due to the T^4 dependence of the blackbody source term, it would be expected that all else being equal that FDS predictions would be high by 30 %. The radiation model predictions are consistent with the other predicted quantities.

The third test modeled was a 440 kW fire. During this test fairly large concentrations of CO were measured along with a much greater amount of external burning. Flames filled the compartment doorway with the exception of a “tunnel” of ambient air going from the lower doorway towards the burner. This test represented the largest test that could be safely run in the VTFRL facility. FDS results are compared to the measured data in Table 3. The same comments regarding the heat flux gauges and gas concentrations apply to this test as for the 270 kW test.

3. Results for the 440 kW Fire

| Parameter | VTFRL | FDS | Parameter | VTFRL | FDS |
|------------|----------------------|-----------------------|------------------------|--------------|---------|
| Door TC 1 | 117 °C | 102 °C | Room TC 1 | 582 °C | 1200 °C |
| Door TC 2 | 88 °C | 471 °C | Room TC 2 | 641 °C | 1210 °C |
| Door TC 3 | 152 °C | 942 °C | Room TC 3 | 688 °C | 1220 °C |
| Door TC 4 | 400 °C | 1190 °C | Room TC 4 | 734 °C | 1230 °C |
| Door TC 5 | 1010 °C | 1190 °C | Room TC 5 | 826 °C | 1230 °C |
| Door TC 6 | 938 °C | 1180 °C | Room TC 6 | 944 °C | 1240 °C |
| Door TC 7 | 968 °C | 1190 °C | Room TC 7 | 977 °C | 1240 °C |
| Door TC 8 | 764 °C | 1230 °C | Room TC 8 | 962 °C | 1250 °C |
| Door Vel 1 | 4.5 m/s | 3.9 m/s | Door O ₂ 1 | 0.4 % | 0.0 % |
| Door Vel 2 | 4.1 m/s | 4.1 m/s | Door O ₂ 2 | 0.6 % | 0.0 % |
| Door Vel 3 | 2.8 m/s | 3.1 m/s | Door O ₂ 3 | 8.8 % | 0.2 % |
| Door Vel 4 | 1.5 m/s | 2.6 m/s | Door O ₂ 4 | 18.0 % | 0.8 % |
| Door Vel 5 | -1.1 m/s | 0.4 m/s | Door O ₂ 5 | 20.4 % | 13.1 % |
| Room HF 1 | N/A | 314 kW/m ² | Door CO ₂ 1 | 8.2 (11.6) % | 11.2 % |
| Room HF 2 | N/A | 290 kW/m ² | Door CO ₂ 2 | 8.1 (11.1) % | 11.2 % |
| Door HF 1 | 66 kW/m ² | 83 kW/m ² | Door CO ₂ 3 | 5.3 (6.3) % | 11.2 % |
| Door HF 2 | 38 kW/m ² | 43 kW/m ² | Door CO ₂ 4 | 1.2 (1.3) % | 11.0 % |
| | | | Door CO ₂ 5 | 0.1 (0.1) % | 4.2 % |

FDS performance for the 440 kW test was similar to that for the 270 kW. Temperatures inside the fire room, and now in the doorway, are overpredicted and the quantity of oxygen depleted air leaving the fire room is also overpredicted. The heat flux predictions are excellent. The data shows that the measured heat flux to the floor did not vary from the 270 kW to the 440 kW test. Since both tests had the same internal compartment temperatures and external burning, the flame surface and wall surfaces were not much different from the point of view of the heat flux gauges. FDS matches this trend showing only a slight increase in heat flux as indicated in the data. It is also encouraging that the concentration of carbon in combustion products is being predicted well in the uppermost region of the doorway. This would indicate that FDS is predicting the net mass exchange at the doorway reasonably well.

SUMMARY AND CONCLUSIONS

As part of continuing efforts to improve FDS v1.0, a new combustion model using the mixture fraction and a new radiation model using the finite volume method has been added to FDS v1.0. This new combustion model was added in the hope that by adding more physics to the combustion routine, that FDS would be more capable of modeling fires during underventilated combustion. The new radiation model allows for surface to surface and surface to gas radiative exchange and makes use of the chemical information provided by the mixture fraction for determining the local absorption coefficients. The simulations in this paper were performed to determine the predictive capabilities of these two new models

Three compartment fire tests at the VTFRL were simulated: a well ventilated test, a moderately underventilated test, and a highly underventilated test. The new models make excellent predictions for the well ventilated test, including being able to correctly predict the radiation heat transfer to the walls. As the degree of underventilation is increased, the performance of FDS degraded; however, the FDS results for most quantities were still acceptable. The main source of error in the FDS predictions as underventilation increased was the overprediction of the compartment gas temperatures and the overprediction in the size of the upper layer. It would also seem that FDS allows too much combustion to occur inside the compartment. This may result from numerical errors in resolving the mixture fraction gradient near Z_F when a coarse grid is used.

The new radiation model is very successful. It matched the data within 10 % for the small fire and predicted well the large fires once the temperature overprediction was accounted for. Some additional development is still needed; however, involving the best manner to correct the source term for coarse grids and selection of an appropriate pathlength for the determination of the absorption coefficient.

The mixture fraction model was relatively successful. For well ventilated tests it is making excellent predictions once the effects of the grid are accounted for. For underventilated tests the predictive quality decreases. There are perhaps two factors contributing to this. The first is that the current state relations do not include minor combustion products such as CO. Including these species would lower the effective heat of combustion and result in an increased volume of gas which would act to force unburned fuel out of the compartment, further reducing the in-compartment heat release. A second factor may lie within the combustion term's numerical discretization. For the well ventilated tests the average mixture fraction near the burner is lower than for the underventilated tests. This results in changing the mixture fraction gradient in the combusting cells. This may result in artificially increasing the heat release due to the coarse noding. If the flame sheet was actually being predicted, then the combusting cell gradients would not differ as much as the flame surface size would differ. More work is needed to reduce errors for coarsely noded grids. The inclusion of soot, CO, and other minor species in the state relations should be explored.

Taken together the new submodels enhance FDS's capabilities without a significant impact on the computational requirements. The finite volume radiation model performs better than the original model which only performed well for small fires in enclosures. The mixture fraction model performs well for small fires, but does not perform as well for larger fires.

However, its performance for larger fires is the same or better than the original model with the added benefit of combustion product information without the time consuming need to track individual species. The mixture fraction model, therefore, also represents an improvement over the original model.

ACKNOWLEDGEMENTS

The efforts of a number of people made this work possible. A few are acknowledged here: Kevin McGrattan of NIST who is the primary developer of the FDS software, Simo Hostikka of VTT, Finland for adding the finite volume radiation model to FDS, and Paul Fuss of NIST for his guidance and assistance in using the RADCAL software for generating absorption coefficients for the finite volume radiation calculation.

REFERENCE LIST

1. McGrattan, K., Baum, H., Rehm, R., Hamins, A., and Forney, G., "Fire Dynamics Simulator - Technical Reference Guide," National Institute of Standards and Technology, NISTIR 6467, 2000.
2. Floyd, J., "Evaluation of the Predictive Capabilities of Current Computational Methods for Fire Simulation in Enclosures Using the HDR T51 and T52 Tests With a Focus on Performance-Based Fire Codes," Ph.D. Dissertation, University of Maryland, 2000.
3. Mell, W., McGrattan, K., and Baum, H., "Numerical Simulation of Combustion in Fire Plumes", Proceedings of the 26th International Symposium on Combustion, Combustion Institute, 1996, pp. 1523-1530.
4. Mahalingam, S., "Analysis and Numerical Simulation of a Nonpremixed Flame in a Corner," Combustion and Flame, Vol. 118, 1999, pp. 221-232.
5. Raithby, G. and Chui, E. "A Finite-Volume Method for Predicting Radiant Heat Transfer in Enclosures with Participating Media," Journal of Heat Transfer, Vol. 112, 1990, pp. 415-423.
6. Wieczorek, C., McKay, C., Vandsburger, U., and Lattimer, B., "Species Formation Using n-Hexane Fires in a Scaled ISO Compartment," NIST Annual Conference on Fire Research, 1998, pp. 103-104.
7. Grosshandler, W., "RADCAL: A Narrow-Band Model for Radiation Calculations in a Combustion Environment," National Institute of Standards and Technology, NIST Technical Note 1402, 1993.
8. Gann, R., Babrauskas, V., and Peacock, R., "Fire Conditions for Smoke Toxicity Measurements," Fire and Materials, Vol. 18, 1994, pp. 193-199.
9. Blevins, L., "Behavior of Bare and Aspirated Thermocouples in Compartment Fires," Proceedings of the 33rd National Heat Transfer Conference, HTD99-280, 1999.
10. Lattimer, B., "The Transport of High Concentrations of Carbon Monoxide to Locations Remote from the Burning Compartment," Thesis, Virginia Polytechnic Institute and State University, 2000.
11. Karlsson, B. and Quintiere, J., "Enclosure Fire Dynamics," CRC Press, 2000.
12. Baum, H., McGrattan, K., and Rehm, R., "Three Dimensional Simulations of Fire Plume Dynamics," Proceedings of the 5th International IAFSS Symposium, Fire Safety Science, 1997, pp. 511-522.